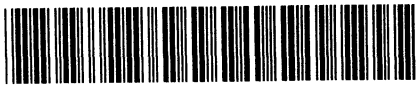

Ref.TH.1306-CERN

THE STRUCTURE OF t CHANNEL EXCHANGES IN KN SCATTERING

F. Elvekjaer
CERN - Geneva

and

B.R. Martin
University College, London

A B S T R A C T

Recent phase shift solutions are used to evaluate KN FESR integrals in order to examine zeros and phases of the t channel exchange amplitudes in the most model-independent way. The results suggest that the line reversal breaking in KN CEX observed for $p_L \lesssim 5.5$ GeV/c is due to a large EXD breaking component in the A_2 exchange flip amplitude. The ρ exchange flip amplitude is well described by a Regge pole amplitude with NWSZ at $-t \approx \approx 0.5$ $(\text{GeV/c})^2$. The imaginary parts of ρ and ω exchange non-flip amplitudes are both peripheral.

Ref.TH.1306-CERN
23 January 1974

1. - INTRODUCTION

One of the interesting features of Regge theory is the concept of exchange degeneracy (EXD), and, in particular, it has often been claimed that $\rho - A_2$ EXD for the (helicity) flip amplitudes is well borne out by data. The systematics of dips in πN and KN charge exchange (CEX) differential cross-sections are among the suggestive features in support of this view [1].

The main characteristics of ρ exchange, as deduced from πN scattering, directly by amplitude analysis [2),3)] and indirectly via finite energy sum rules (FESR) [4], are : the imaginary part of the non-flip amplitude has cross-over zeros at $-t \approx 0.2$ and 1.2 GeV/c)^2, as required by peripherality or the dual absorptive model [5] ; the real and imaginary parts of the flip amplitude have Regge pole behaviour up to t values as large as $-t \approx 2.5$ (GeV/c)^2. Hence ρ exchange amplitudes are peripheral for $-t \lesssim 1.0$ (GeV/c)^2.

A_2 exchange has been studied via FESR's for $\gamma N \to \pi N$ [6] and $\pi^- p \to \eta^o n$ [7] and by differential cross-sections for $\pi^- p \to \eta^o n$ [8] and $\pi^+ p \to \eta^o \Delta^{++}$ [9]. Here one sees evidence for Regge pole dominance of the flip amplitude, in particular from the dip at $-t \approx 1.5$ (GeV/c)^2 in the cross-section data. Determination of the effective A_2 trajectory [10] does, however, suggest that A_2 exchange has features different from those of ρ exchange. Data in the region of 4 GeV/c [11] indicate that the $K^+ n \to K^o p$ differential cross-section is larger than that for $K^- p \to \bar{K}^o n$ by up to a factor of 2 for $-t \lesssim 0.6$ (GeV/c)^2. This implies either that $\rho - A_2$ EXD is broken for the flip amplitudes or that the non-flip amplitudes are of the same order of magnitude as the flip amplitudes in this energy range.

Another warning that the nature of tensor exchanges might be different from that of vector exchanges is given by the study of f exchange in πN scattering by Barger et al. [12]. This work indicated a non-peripheral structure of f exchange amplitudes. On the other hand, Davier [13] has given arguments in favour of a peripheral f. These two studies were based on different assumptions on the Pomeron amplitude. The same kind of confusion exists for the K* tensor exchange, K_T^*. In the analysis of hypercharge exchange reactions at 4 and 14 GeV/c by Irving et al. [14] it was assumed that EXD works for flip amplitudes and they found a non-peripheral K_T^* amplitude. Fits to hypercharge-exchange data have, however, been successfully made with peripheral amplitudes [15].

To separate specific t channel exchanges, (P+f), A_2, ρ and ω, requires knowledge of both KN and $\bar{K}N$ amplitudes for I = 0 and 1. The recently published phase shifts for I = 0 KN scattering [16] completes the set of necessary amplitudes in the phase shift region ($p_L \lesssim 1.5$ GeV/c), and thus makes the separation possible.

We have in this work evaluated low energy parts (left-hand sides) of FESR's involving both the real and imaginary parts in order to examine zeros and phases of the different amplitudes in the most model-independent way. This is much in the same spirit as in the earlier work of Dass and Michael [17]. At that time, however, they had available only $K^{\pm}p$ phase shifts, and also the KNY coupling constants were very poorly known. In addition to separating all the exchanges we have also tried to improve the extrapolation of real parts, and at the same time, to extend the analysis to $-t \simeq 1.5$ $(GeV/c)^2$.

The main conclusions are :

(i) the ρ exchange flip amplitude is well described by a Regge pole model ;

(ii) the imaginary parts of ρ and ω exchange non-flip amplitudes are peripheral ;

(iii) A_2 exchange is dominated by the flip amplitude ; the low energy phase shifts are not compatible with ρ-A_2 EXD for the flip amplitudes ; the breaking is in the same direction as suggested by data on KN and $\bar{K}N$ CEX in the 4 GeV/c region. Neither the flip nor the non-flip A_2 amplitude is peripheral.

The line reversal breaking for KN and $\bar{K}N$ CEX thus seems to be almost entirely due to a large EXD breaking component in the A_2 exchange flip amplitude. Although present at 4 GeV/c the line reversal breaking might disappear at higher energies as is suggested by data at 5.5 and 12 GeV/c [18].

We have, of course, the usual problem of separating the P and f amplitudes, and the ω exchange flip amplitude appears not to be well determined by the data. The preferred solution has the flip amplitudes for both (P+f) and ω exchange small, the latter in accordance with the lack of a forward turnover in the differential cross-section for $K_L^o p \to K_S^o p$ [1].

2. - FESR's FOR KN SCATTERING

2.1. - The information content of FESR integrals

In the following we will work at fixed t with invariant s channel helicity amplitudes $F_{+\pm}(\nu) \equiv \nu^n f_{+\pm}(\nu)$ corresponding to definite t channel exchange quantum numbers. Powers of ν are introduced to ensure that $F(\nu)$ (dropping the subscripts) is odd under crossing,

$$F(\nu) = -F(-\nu) \tag{2.1}$$

[Here ν is the usual crossing variable $\nu = (s-u)/(4M)$ and M is the nucleon mass.] For ρ and ω exchange, $n = 0$, and for $(P+f)$ and A_2 exchange, $n = 1$.

$F(\nu)$ is a real analytic function, and we will consider the low energy part, L_γ, of the FESR integrals for different moments γ,

$$L_\gamma \equiv \int_0^N d\nu \; \mathrm{Im}\{ w_\gamma(\nu^2) F(\nu) \} \tag{2.2}$$

and weight functions

$$w_\gamma(\nu^2) = (\bar{\nu}^2 - \nu^2)^\gamma \tag{2.3}$$

N is taken as the upper limit of the phase shift region, and the Born terms are included in the integral. The precise choice of the branch point $\bar{\nu}(< N)$ of $w_\gamma(\nu^2)$ is related to the problem of continuation of Re F to large $-t$, and we will discuss this in Section 2.2 below.

The idea of evaluating the L_γ's is that they contain information on $F(\nu)$ for $\nu \gtrsim N$. The phase shift information only extends to $p_L \approx 1.5$ GeV/c, which is rather a low cut-off. However, KN scattering is rather featureless above 1.0 GeV/c, and all the prominent peaks in the $\bar{K}N$ total cross-sections are covered by this region, so we may hope that in practice the cut-off is high enough. We are further encouraged in this view by results in πN scattering, which show that even though the cut-off energy is low, and the phase shifts may be <u>locally</u> wrong, it is reasonable to expect the FESR integrals to contain <u>general</u> features of the amplitudes at higher energies. In the case where $F(\nu) \sim \nu^\alpha$ for $\nu \gtrsim N$ (Regge pole behaviour) one would have

$$\mathrm{Im}\{w_\gamma(\nu^2)F(\nu)\} \simeq \frac{\alpha+2\gamma+1}{N}\left(\frac{\nu}{N}\right)^{\alpha+2\gamma} L_\gamma \,, \quad \nu \gtrsim N \tag{2.4}$$

and L_γ with γ = integer would yield information on Im F, and with γ = half-integer would give information on Re F, for $\nu \gtrsim N$.

We do not expect all the amplitudes to be well approximated by Regge pole forms, and without a specific model we cannot arrive at a simple result like (2.4). We will assume, however, that from L_γ one can still deduce features like the order of magnitude of F, and also roughly what its phase should be, e.g., in which quadrant it lies. Any fixed t zeros of F will, of course, show up in L_γ.

2.2. - Convergence and weight functions

To perform the integration in Eq. (2.2) we need the amplitude at large -t in the unphysical region, see Fig. 1. For γ = integer, we only need Im F. For γ = half-integer we need Im F for $\nu^2 < \bar{\nu}^2$ [see Eq. (2.3)], and Re F for $\nu^2 > \bar{\nu}^2$. We have chosen to use the conventional Legendre series expansions for the extrapolations. The convergence of these are, strictly speaking, very limited, and governed by the boundaries of the double spectral functions. In particular, Re F is only convergent for $|t| \lesssim 4m_\pi^2$ (m_π = pion mass). In addition, for $-t \gtrsim 0.95$ (GeV/c)^2 the s channel and the u channel cuts overlap. For the last problem we arrange $\bar{\nu}^2$ to be large enough so that $w_\gamma(\nu^2)$ is real in the overlapping cut region. We therefore need only Im F, which in this region is given by [recall that $F(\nu)$ is odd under crossing]

$$\mathrm{Im}\,F(\nu+i\varepsilon,t) = \mathrm{Im}\,F_s(\nu+i\varepsilon,t) + \mathrm{Im}\,F_s(-\nu+i\varepsilon,t) \tag{2.5}$$

where $\mathrm{Im}\,F_s(\nu,t)$ denotes the physical region imaginary part continued to the point (ν,t).

The extrapolation of F to large -t is, as mentioned, restricted by the boundaries of the double spectral functions. The latter can be calculated from box diagrams with the lowest mass states inserted in the loops, as described by Mandelstam [19]. [The explicit graphs have been given by Lee [20].]

These boundaries are labelled a, b, c,..., h on Fig. 1. Although these are the strict double spectral function boundaries, it is likely that the first effective boundaries are given by box graphs with the $\pi\pi$ and πK intermediate states replaced by resonances at the ρ and K*(890) masses, respectively. The resulting boundaries are labelled a', b', c',..., h' on Fig. 1, and they are so far from the region of interest in the Mandelstam plane that it is probably reasonable to use Legendre series expansions for the extrapolation of Im F out to $-t \simeq 1.5$ (GeV/c)^2. For Re F, however, the convergence is still, in principle, limited to $|t| \lesssim 4m_\pi^2$, the asymptotic limit of the boundary b' being at $t = 4m_\pi^2$. For this reason, we have chosen to work with the branch point $\bar{\nu}$ of w_γ given by

$$\bar{\nu} = \nu_1(t) \tag{2.6}$$

where $\nu_1(t)$ is the ν value at the physical boundary $t = -4q^2$ (q = centre-of-mass momentum). This ensures that we need Re F only in the physical region.

To check that our results are not dependent on this choice of weight function we have also tried to use the branch point at $\bar{\nu} = \nu_2(t)$ where $\nu_2(t)$ is evaluated at the fixed s value $s = 2.6$ (GeV/c)^2. This value of s ensures that the weight function for $-t \lesssim 1.5$ (GeV/c)^2 is real in the region where the s and u channel cuts overlap. This weight function of course requires Re F at large $-t$ and the extrapolation by Legendre series only makes sense if we make some additional assumptions on the strength of the double spectral functions. We have nevertheless applied this method with the modification that the Born terms are treated separately. Obviously it does not make sense to approximate the Born terms by a small number of partial waves when one is near the pole position. We have therefore subtracted the partial waves of the Born terms from the partial waves as given by the phase shift solutions in the physical region and the Born terms have been extrapolated explicitly. We found that none of the qualitative features of the L_γ's obtained with the choice $\bar{\nu} = \nu_1(t)$ Eq. (2.6), were changed if we used $\bar{\nu} = \nu_2(t)$ as described in this section.

3. - FORMALISM AND DATA

3.1. - Formalism

To leading order in s, the invariant s channel helicity flip and non-flip amplitudes $f_{+\pm}$ are given by

$$f_{++} = A + \nu B \quad ; \quad f_{+-} = A \tag{3.1}$$

where A and B are the usual invariant amplitudes [see, e.g., Ref. 21].

In terms of t channel exchange amplitudes we use the convention (helicity indices suppressed)

$$\begin{aligned}
f(K^- p) &= f(P) + f(f) + f(A_2) + f(\rho) + f(\omega) \\
f(K^+ p) &= f(P) + f(f) + f(A_2) - f(\rho) - f(\omega) \\
f(K^- n) &= f(P) + f(f) - f(A_2) - f(\rho) + f(\omega) \\
f(K^+ n) &= f(P) + f(f) - f(A_2) + f(\rho) - f(\omega) \\
f(K^- p \to \bar{K}^0 n) &= 2f(A_2) + 2f(\rho) \\
f(K^+ n \to K^0 p) &= 2f(A_2) - 2f(\rho)
\end{aligned} \tag{3.2}$$

where f(KN) is the elastic KN → KN amplitude, and likewise for $f(\bar{K}N)$.

The crossing odd amplitudes of Eq. (2.1) are

$$F(P) = \nu f(P) \ , \ F(f) = \nu f(f) \ , \ F(A_2) = \nu f(A_2),$$
$$F(\rho) = f(\rho) \ , \ F(\omega) = f(\omega) \ . \tag{3.3}$$

3.2. - Data input

The helicity amplitudes $F(\nu)$ of Eq. (3.3) are constructed via the decompositions of Eq. (3.2) and the relations (3.1) using as input partial wave amplitudes for KN and $\bar{K}N$ scattering with I = 0 and 1, and the values of the $KN\Lambda$ and $KN\Sigma$ coupling constants.

Several phase shift analyses exist of $I = 1$ $\bar{K}N$ scattering (K^+p), the most extensive of which is that of Albrow et al. [22]. This analysis produced three solutions, the so-called Sens α, β and γ solutions, and one of these, Sens γ, has subsequently been shown to give the best over-all fit to recent high statistics K^+p elastic differential cross-section measurements [23]. Furthermore, the threshold S and P waves of this solution are consistent with forward dispersion relations [24]. We have therefore used the Sens γ solution as an input for the $I = 1$ $\bar{K}N$ channel. However, we have also examined the use of the Sens β solution, as this has some partial waves qualitatively different from those of solution γ, and gives a fit to the data of Ref. 23) which is not too inferior.

Far less work has been done on the $I = 0$ $\bar{K}N$ channel, but recently an extensive phase shift analysis of data obtained from K^+d interactions has been published [16]. Two basic families of solutions are presented, one of which is preferred by virtue of its detailed fit to the data. For example, it alone predicts the correct sign for the sole measurement of the K^+n charge-exchange polarization at 600 MeV/c. [Other reasons for preferring this type of solution are given in Ref. 16).] For convenience we used an energy-dependent member of this family, and for consistency with our $I = 1$ $\bar{K}N$ input we used the $I = 0$ solution which was obtained using the Sens γ $I = 1$ amplitudes as input to the K^+d phase shift analysis. Thus we have used the so-called BGRT-D (Sens γ) solution. This solution also has threshold amplitudes qualitatively consistent with forward dispersion relations [24].

The upper limit of the $I = 0$ $\bar{K}N$ phase shift analysis [16], $p_L = 1.5$ GeV/c, dictates the cut-off in the FESR integrals. However, although $\bar{K}N$ phase shift analyses have been made up to (and beyond) this momentum, no up-to-date analyses exist of the entire region, and we are therefore forced to use amplitudes from different analyses. This raises possible problems of continuity which we will discuss in Section 3.3 below.

We start with the very low energy region $p_L \lesssim 0.43$ GeV/c, and the unphysical region below the $\bar{K}N$ threshold. Several K matrix analyses have been made of this region, all of which agree reasonably well in the physical region, but differ substantially when extrapolated into the unphysical region. One of these is the SPD wave analysis of Kim [25], which on extrapolation yields a $\Lambda(1405)$ resonance with width ≈ 50 MeV, in agreement with production data [26], and a strong coupling to the $\bar{K}N$ channel

(as measured, for example, by the imaginary part of the S wave I = 0 $\bar{K}N$ elastic amplitude below the $\bar{K}N$ threshold), and a $\Sigma(1385)$ state essentially decoupled from $\bar{K}N$. In contrast, Chao et al. [27] have published an S wave solution which also has a $\Lambda(1405)$ with width ≈ 50 MeV, but much smaller coupling to the $\bar{K}N$ channel. Lacking any definite evidence in favour of either, we have used both solutions as input to the FESR integrals. In practice, only the S and P waves of Kim were used, and the S waves of Chao et al. were supplemented by a $\Sigma(1385)$ state with coupling given by SU(3), for which there is some independent evidence [28] (in contrast to the result of Kim which gives this coupling very small). Finally to both solutions was added a $\Lambda(1520)$ resonance of standard Breit-Wigner form, including barrier factors of the type used by Litchfield et al. [29], and with parameters as given in Ref. 26).

The next region which has been studied is $0.43 \leq p_L \lesssim 1.2$ GeV/c where there exist two recent multi-channel phase shift analyses, those of Langbein and Wagner (LW) [30] and Lea et al. (LOMM) [31]. Although analyzing essentially the same data these two solutions have substantial differences both in their resonance spectra and in details of branching ratios. We have, therefore, included both *) as input to the FESR's, although we shall comment on some difficulties with the LW solution below.

Finally, there remains the region $1.2 \leq p_L \leq 1.5$ GeV/c. The most extensive analysis here is that of Litchfield et al. [29], and we have used this exclusively.

In addition to KN and $\bar{K}N$ low energy amplitudes we also need the values of the $KN\Lambda$ and $KN\Sigma$ coupling constants. For a long time these have been a source of uncertainty in all calculations in low energy KN physics. Early attempts to determine them from KN forward dispersion relations proved unreliable owing to the sensitivity of the methods to the poorly known $\Lambda(1405)$ parameters [21], and recent work has concentrated on more model-independent methods. The most reliable of these calculations is probably that of Pietarinen and Knudsen [32], which uses modern methods of analytic continuation and avoids using the poorly known KN forward real parts.

---

*) In practice we have used an improved version of the published LOMM solution which includes the correct threshold behaviour for the partial wave amplitudes.

We have therefore used their value of $G^2 \equiv g^2_{KN\Lambda}/4\pi + g^2_{KN\Sigma}/4\pi$ and assumed that the ratio $g_{KN\Lambda}/g_{KN\Sigma}$ is given approximately by SU(3) with mixing parameter $\alpha = 2/3$. Thus we have used $g^2_{KN\Lambda}/4\pi = 11.0$, $g^2_{KN\Sigma}/4\pi = 1.4$.

We will distinguish solutions in what follows by their combination of amplitudes in the $\bar{K}N$ channel and denote them : Chao et al.-LW (A), Chao et al.-LOMM (B), Kim-LW (C), and Kim-LOMM (D).

3.3. - Continuity in energy

Before embarking on the evaluation of the FESR integrals we have to consider the continuity of the input amplitudes as a function of s.

In the KN channel there is no problem. The $I = 0$ input is an explicitly energy-dependent analysis and therefore smooth. The $I = 1$ KN input is from an energy-independent analysis, but the quality of the K^+p data is such that the dominant partial wave amplitudes are also very smooth as functions of s.

The situation is not so simple in the $\bar{K}N$ channel where our input is not all taken from the same source. We have therefore reconstructed the invariant helicity amplitudes $\bar{f}^I_{+\pm}(s,t)$ for $\bar{K}N$ scattering $(I = 0,1)$ and examined their continuity as functions of s for fixed values of t in the range of interest. For solutions (B) and (D) (i.e., those using the LOMM amplitudes) the amplitudes are, of course, smooth, as they all come from energy-dependent analyses, and so we have only to consider the matching of the two regions at $p_L \approx 0.43$ GeV/c and ≈ 1.2 GeV/c. We find that this matching is excellent for the $I = 0$ amplitudes $\bar{f}^0_{+\pm}$ and the imaginary parts of the $I = 1$ amplitudes, but somewhat worse for the real parts, particularly $\mathrm{Re}\,\bar{f}^1_{+-}$ for input (D). However, the $I = 1$ amplitudes are in general somewhat smaller than those for $I = 0$ and so a small mismatch at the joints will have a negligible effect. (In practice, the different regions were joined by smooth interpolations.) As examples, we show in Fig. 2a-2c $\bar{f}^0_{+-}$ and $\mathrm{Re}\,\bar{f}^1_{++}$ at $t = 0$ from input (B). For inputs (A) and (C) (i.e., those using the LW amplitudes) only $\bar{f}^0_{+-}$ and $\mathrm{Im}\,\bar{f}_{++}$ have excellent matching. For input (A) all other amplitudes have small (but acceptable) mismatches similar to those present in $\mathrm{Re}\,\bar{f}^1_{+\pm}$ for (B) and (D). For input (C), however, there are more serious mismatches in $\mathrm{Re}\,\bar{f}^1_{+\pm}$.

An additional difficulty with inputs (A) and (C) is that the LW analysis is energy-independent, and the reconstructed amplitudes often show considerable residual scatter. For example, in Fig. 2d we show Re $\bar{f}^1_{+-}$ at $t = 0$ from input (C). Away from $t = 0$ this problem tends to become more severe.

From over-all continuity considerations the inputs in order of preference are (B), (D), (A), (C).

4. - RESULTS

In Fig. 3, we show for $0 \leq -t \leq 1.5$ $(GeV/c)^2$ the values of L_0 and $L_{\frac{1}{2}}$ corresponding to weight functions w_γ with threshold $\bar{\nu} = \nu_1$, see Eqs. (2.2), (2.3) and (2.6). The labels (A), (B), (C), (D) refer to different $\bar{K}N$ phase shift solutions as explained in the previous section, and the $I = 1$ KN input is Sens γ. No qualitative differences are found in the FESR integrals if the Sens γ solution is replaced by the Sens β solution. The reason why we show only the moments $\gamma = 0, \frac{1}{2}$ is that we believe these are the most reliable ones. It is clear that by choosing very high or very low moments one would heavily weight either the upper or the lower end of the integration region. By choosing the moments $\gamma = 0, \frac{1}{2}$ one tries to weight information in the whole region evenly. We have produced all the L_γ's with $\gamma = 0, \frac{1}{2}, \ldots, \frac{5}{2}$ and although quantitative differences do exist, all the qualitative features to be discussed below proved to be unchanged. We have also checked that these features are stable against changes in the cut-off between $p_L = 1.2$ and 1.5 GeV/c. As discussed in Section 2.2, the results do not depend on our particular choice of weight function.

We will now discuss each exchange separately.

4.1. - ρ exchange

The flip amplitude $F_{+-}(\rho)$ exhibits (like in πN charge exchange) pure Regge pole behaviour, with wrong signature nonsense zeros corresponding to a linear ρ trajectory α_ρ [both zeros and phase consistent with $\alpha_\rho / \Gamma(1+\alpha_\rho)[\mathrm{tg}(\pi \alpha_\rho/2) + i]$]. The real part has a double zero at $-t \approx 0.3 - 0.5$ *) and the imaginary part a single zero

---

*) Here, and in the following, t is given in units $(GeV/c)^2$.

at $-t \approx 0.5$. Since $\mathrm{Im}\, w_{\frac{1}{2}}(\nu^2) < 0$ for $\nu^2 > \bar{\nu}^2$ the ρ flip amplitude is in the third quadrant in the complex plane [see Eq. (2.4)].

The non-flip amplitude $F_{++}(\rho)$ has the cross-over zero in the imaginary part at $-t \simeq 0.2$ and a second zero at larger $-t$. The uncertainty in $\mathrm{Im}\, F_{++}(\rho)$ for $-t \gtrsim 0.5$ is due almost entirely to differences in the unphysical region of the $\bar{K}N$ input, in particular the strength of the $\Sigma(1385)$ effective coupling. For inputs using the Kim solution the second zero is at $-t \approx 1.2$ as required by the dual absorptive model. $\mathrm{Re}\, F_{++}(\rho)$ has the same general trend as given by πN amplitude analysis. It has a zero which has moved out to larger $-t$ (≈ 1.0).

As in the πN case $|F_{+-}(\rho)| \gg |F_{++}(\rho)|$.

4.2. - ω exchange

The ω non-flip amplitude $F_{++}(\omega)$ has a similar structure to $F_{++}(\rho)$, and like the latter the uncertainties for $-t \gtrsim 0.5$ are due mainly to the differences in the unphysical region of the $\bar{K}N$ input. If we use inputs (C) and (D) (i.e., the Kim solution for the unphysical region) then $F_{++}(\omega)$ and $F_{++}(\rho)$ are almost identical.

The flip amplitude $F_{+-}(\omega)$ is very poorly determined by the data and one cannot make any definite conclusions about this amplitude. It is interesting to note, however, that for the inputs preferred from continuity considerations, i.e., (B) and (D) $F_{+-}(\omega)$ is very small in the near forward direction which is in accord with the lack of forward turnover in the $K_L^0 p \to K_S^0 p$ differential cross-section at high energies [1].

4.3. - A_2 exchange

As expected, the flip amplitude is much larger than the non-flip amplitude $|F_{+-}(A_2)| \gg |F_{++}(A_2)|$.

Given that $F_{+-}(\rho)$ is well described by a Regge pole, and assuming exchange degeneracy, one would expect $F_{+-}(A_2)$ to lie in the fourth quadrant in the complex plane for $-t \lesssim 0.5$. From Fig. 3 it is clear that it lies in the first quadrant. Hence it follows that ρ-A_2 exchange degeneracy for the flip amplitudes does not work down to the phase shift region.

It is interesting to note that this is supported by the KN and $\bar{K}N$ charge exchange differential cross-section data in the 4 GeV/c region [11]. The amplitudes for $K^+n \to K^0p$ and $K^-p \to \bar{K}^0n$ are given by the difference and the sum of the ρ and A_2 exchange amplitudes, respectively, see Eq. (3.2). From our result one would expect the differential cross-section for $K^+n \to K^0p$ to be larger than that of $K^-p \to \bar{K}^0n$ for $-t \lesssim 0.5$. This is in accordance with the data at 4 GeV/c, which have the former larger than the latter by up to a factor of two for $-t \lesssim 0.6$.

We note that $\mathrm{Im}\, F_{+-}(A_2)$ seems to be maximal where peripherality or the dual absorptive model would require a zero. The dip in the differential cross-section at $-t \simeq 1.5$ for $\pi^-p \to \eta^0n$ and $\pi^+p \to \eta^0\Delta^{++}$ [9),10)] is in nice agreement with the minimum of $F_{+-}(A_2)$ at this t value suggested by the FESR integrals.

The imaginary part of the non-flip amplitude $F_{++}(A_2)$ is one of the smaller amplitudes. It is, however, of the same order of magnitude as $F_{++}(\rho)$ and $F_{++}(\omega)$ and it does not show the dual absorption model zero.

4.4. - <u>(P + f) exchange</u>

As usual we cannot separate these two exchanges and we only make the following very qualitative statements.

Firstly it does not seem to be from the FESR integrals a well justified assumption that (P + f) exchange is predominantly non-flip and imaginary, except in the very forward region. This assumption is an essential ingredient in the argument in favour of ρ-A_2 exchange degeneracy from the $K^{\pm}p$ polarization data. Our result is in qualitative agreement with the amplitude analysis of πN scattering of Ref. 3). Here it is shown that the non-flip (P + f) amplitude even at 14 GeV/c has a substantial real part.

Finally it might be interesting to note that $F_{+-}(P + f)$ has a shape similar to that of $F_{+-}(A_2)$. With the assumption that $F_{+-}(P)$ has no essential structure it becomes plausible that f exchange is similar to A_2 exchange. In view of the results for ρ and ω exchange this might suggest that tensor exchange is different in nature from vector exchange.

ACKNOWLEDGEMENTS

It is a pleasure to acknowledge valuable discussions with R.C. Johnson, C. Michael, G.C. Oades, R.J.N. Phillips and B. and F. Schrempp. One of us (F.E.) wants to thank for kind hospitality at Rutherford Laboratory where part of this work was performed.

REFERENCES

1) See, e.g. :
C. Michael - in Proceedings of the Oxford Conference on High Energy Collisions (1972) ;
R.J.N. Phillips - in Proceedings of the Amsterdam Conference on Elementary Particles (1972).

2) F. Halzen and C. Michael - Phys.Letters 36B, 367 (1971) ;
R.L. Kelly - Phys.Letters 39B, 635 (1972) ;
G. Cozzika et al. - Phys.Letters 40B, 281 (1972) ;
R.C. Miller, A. Yokosawa and P. Johnson - Phys.Rev.Letters 30, 242 (1973), and ANL Preprint (1973).

3) F. Elvekjaer, T. Inami and R.J.N. Phillips - Nuclear Phys. B64, 301 (1973).

4) See, e.g. :
V. Barger and R.J.N. Phillips - Phys.Rev. 187, 2210 (1969) ;
F. Elvekjaer, T. Inami and G. Ringland - Phys.Letters 44B, 91 (1973).

5) H. Harari - Ann.Phys. 63, 432 (1971).

6) R. Worden - Nuclear Phys. B37, 253 (1972) ;
See also :
I.M. Barbour and R.G. Moorhouse - CERN Preprint TH. 1712 (1973).

7) J. Harnad - Oxford Ph.D. Thesis, quoted by R.J.N. Phillips in Ref. 1).

8) R. Yamamoto et al. - MIT Preprint 16511 (1973).

9) D.F. Grether and G. Gidal - Phys.Rev.Letters 26, 792 (1971).

10) V.N. Bolotov et al. - Serpukhov Preprint (1973).

11) W. Moninger et al. - Illinois Preprint COO-1195-212 (1972) ;
R. Blokzijl et al. - Nuclear Phys. B51, 535 (1973).

12) V. Barger, K. Geer and F. Halzen - Nuclear Phys. B49, 302 (1972).

13) M. Davier - Phys.Letters 40B, 369 (1972).

14) A.C. Irving, A.D. Martin and V. Barger - Nuovo Cimento 16A, 573 (1973).

15) J.S. Loos and J.A.J. Mathews - Phys.Rev. D6, 2463 (1972) ;
B. Schrempp and F. Schrempp - Private communication.

16) G. Giacomelli et al. (BGRT Collaboration) - CERN Preprint (1973).

17) G.V. Dass and C. Michael - Phys.Rev. 175, 1774 (1968).

18) P. Astbury et al. - Phys.Letters 23, 396 (1966) ;
D. Cline et al. - Nuclear Phys. B22, 247 (1970) ;
A. Firestone et al. - Phys.Rev.Letters 25, 958 (1970).

19) S. Mandelstam - Phys.Rev. 115, 1741 (1959) ; 115, 1752 (1959).

20) B.W. Lee - Ph.D. Thesis, University of Pennsylvania (1960).

21) B.R. Martin - Springer Tracts in Modern Physics 55, 73 (1970).

22) M.G. Albrow et al. - Nuclear Phys. B30, 273 (1971).

23) B.J. Charles et al. - Phys.Letters 40B, 289 (1972) ;
P.C. Barber et al. - Rutherford Laboratory Preprint RPP/H/104.

24) C.P. Knudsen and B.R. Martin - Nuclear Phys. B61, 307 (1973).

25) J.K. Kim - Phys.Rev.Letters 19, 1074 (1967).

26) Particle Data Group - Revs.Modern Phys. 45, 51 (1973).

27) Y.A. Chao, R.W. Kraemer, D.W. Thomas and B.R. Martin - Nuclear Phys. B56, 46 (1973).

28) K.O. Bunnell et al. - Nuovo Cimento Letters 3, 224 (1970) ;
R.D. Tripp et al. - Phys.Rev.Letters 21, 1721 (1968).

29) P.J. Litchfield et al. - Nuclear Phys. B30, 125 (1971).

30) W. Langbein and F. Wagner - Nuclear Phys. B47, 477 (1972).

31) A.T. Lea, G.C. Oades, B.R. Martin and R.G. Moorhouse - Nuclear Phys. B56, 77 (1973).

32) E. Pietarinen and C.P. Knudsen - Nuclear Phys. B57, 637 (1973).

FIGURE CAPTIONS

Figure 1 Mandelstam diagram showing boundaries of the nearest double spectral functions as calculated from box graphs with stable particle intermediate states (a,b,...,h), and nearest effective boundaries using resonances in the loops (a',b',...,h'). s_{max} corresponds to p_L = 1.5 GeV/c and the dotted region is the physical phase shift region.

Figure 2 Phase shift amplitudes at t = 0 as functions of $\sqrt{s}$ in units GeV = c = 1.
(a) Im $\bar{f}^{I=0}_{+-}$; (b) Re $\bar{f}^{I=0}_{+-}$; (c) Re $\bar{f}^{I=1}_{++}$ and (d) Re $\bar{f}^{I=1}_{+-}$.
The phase shift solutions are :
(----) Chao et al. [27] ;
(-x-x) Kim [25] ;
(——) LOMM [31] ;
(●●●) Langbein and Wagner [30] ;
(-.-.) Litchfield et al. [29].

Figure 3 FESR integrals L_γ in units GeV = c = 1. $\gamma = 0$ gives information on imaginary parts (a). $\gamma = \frac{1}{2}$ gives information on real parts (b). The phase shift solutions are labelled according to the choice for the $\bar{K}N$ channel : (A) Chao et al.-Langbein and Wagner ; (B) Chao et al.-LOMM ; (C) Kim-Langbein and Wagner ; (D) Kim-LOMM. The KN phase shifts are the Sensγ solution [22] for I = 1 and BGRT-D (Sens γ) [16] for I = 0. The hatched bands cover all four phase shift combinations unless otherwise indicated.

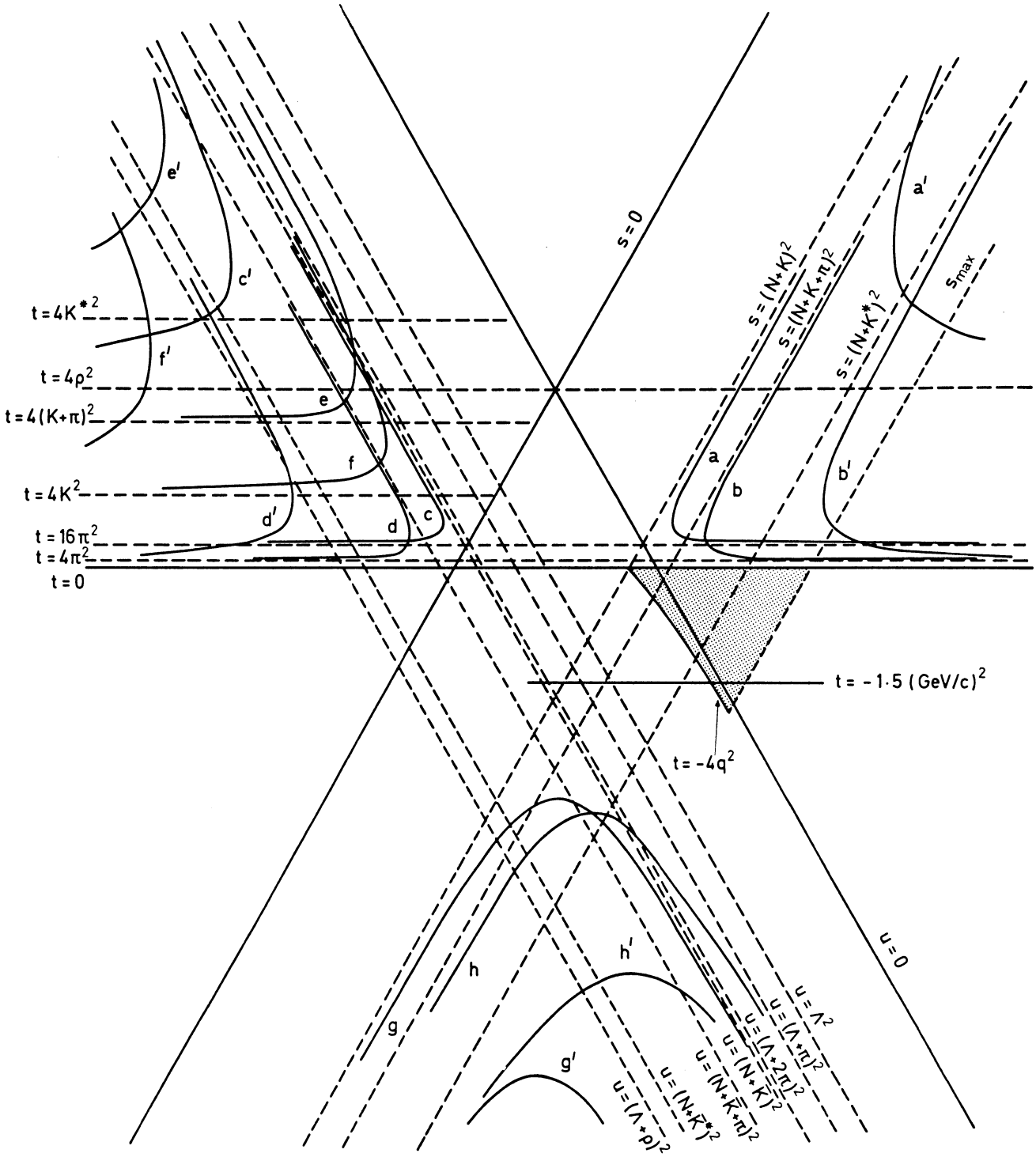
s=0
u=0
t=4K*2
t=4ρ2
t=4(K+π)2
t=4K2
t=16π2
t=4π2
t=0
t=-1.5 (GeV/c)2
t=-4q2
s=(N+K)2
s=(N+K+π)2
s=(N+K*)2
smax
u=Λ2
u=(Λ+π)2
u=(Λ+2π)2
u=(N+K*)2
u=(N+K+π)2
u=(Λ+ρ)2
a
a'
b
b'
c
c'
d
d'
e
e'
f
f'
g
g'
h
h'

- Figure 1 -

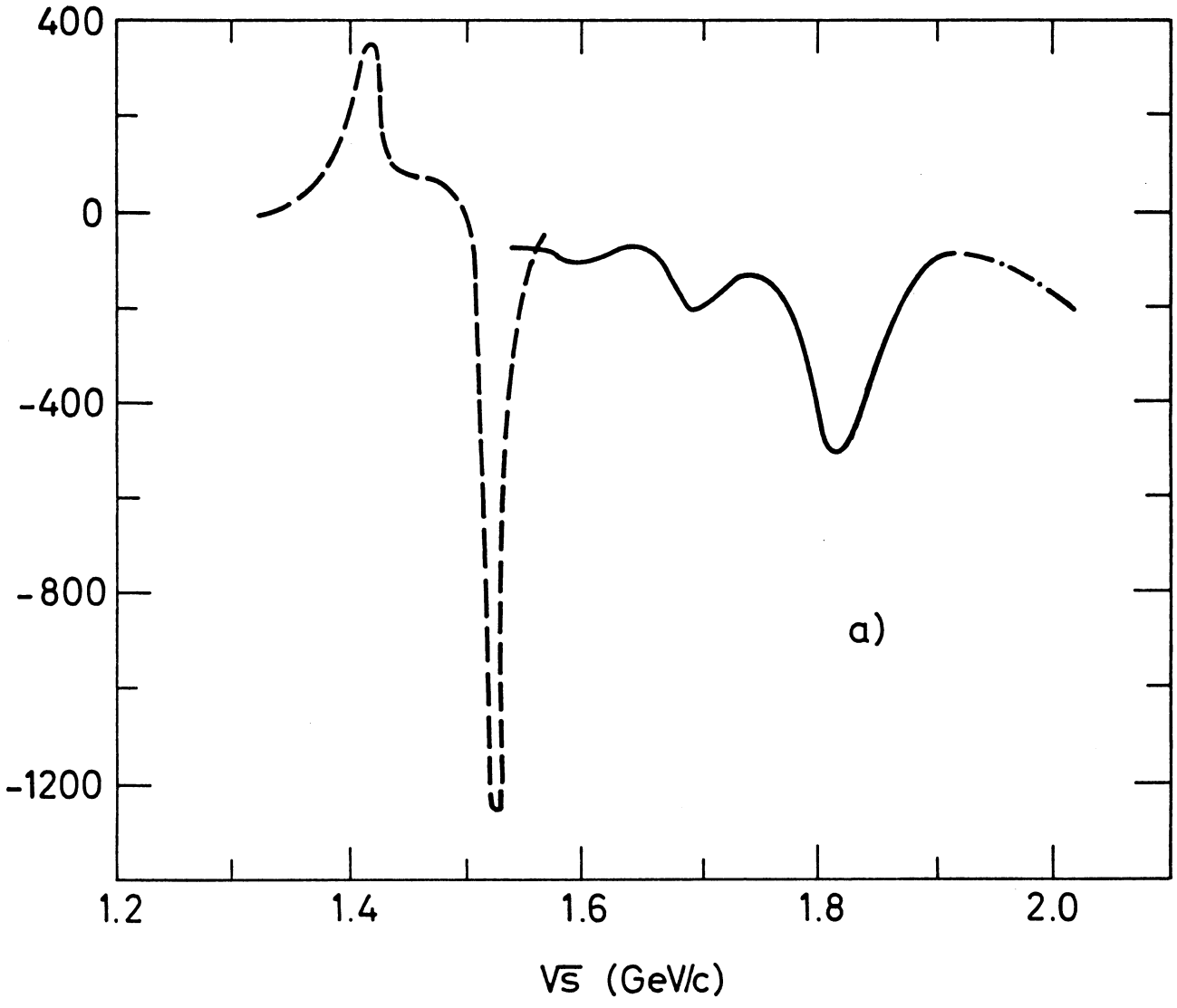

- Figure 2a -

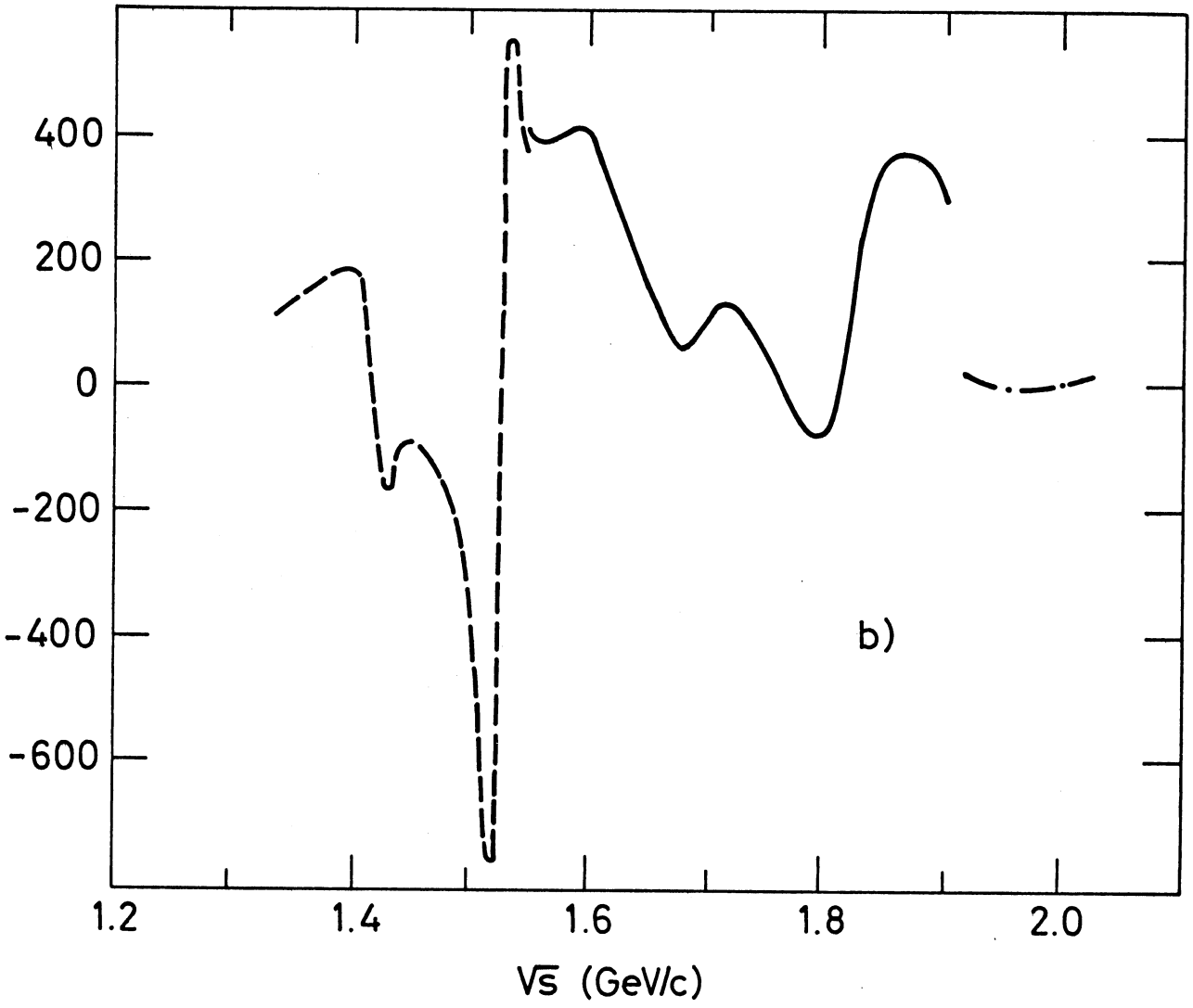

- Figure 2b -

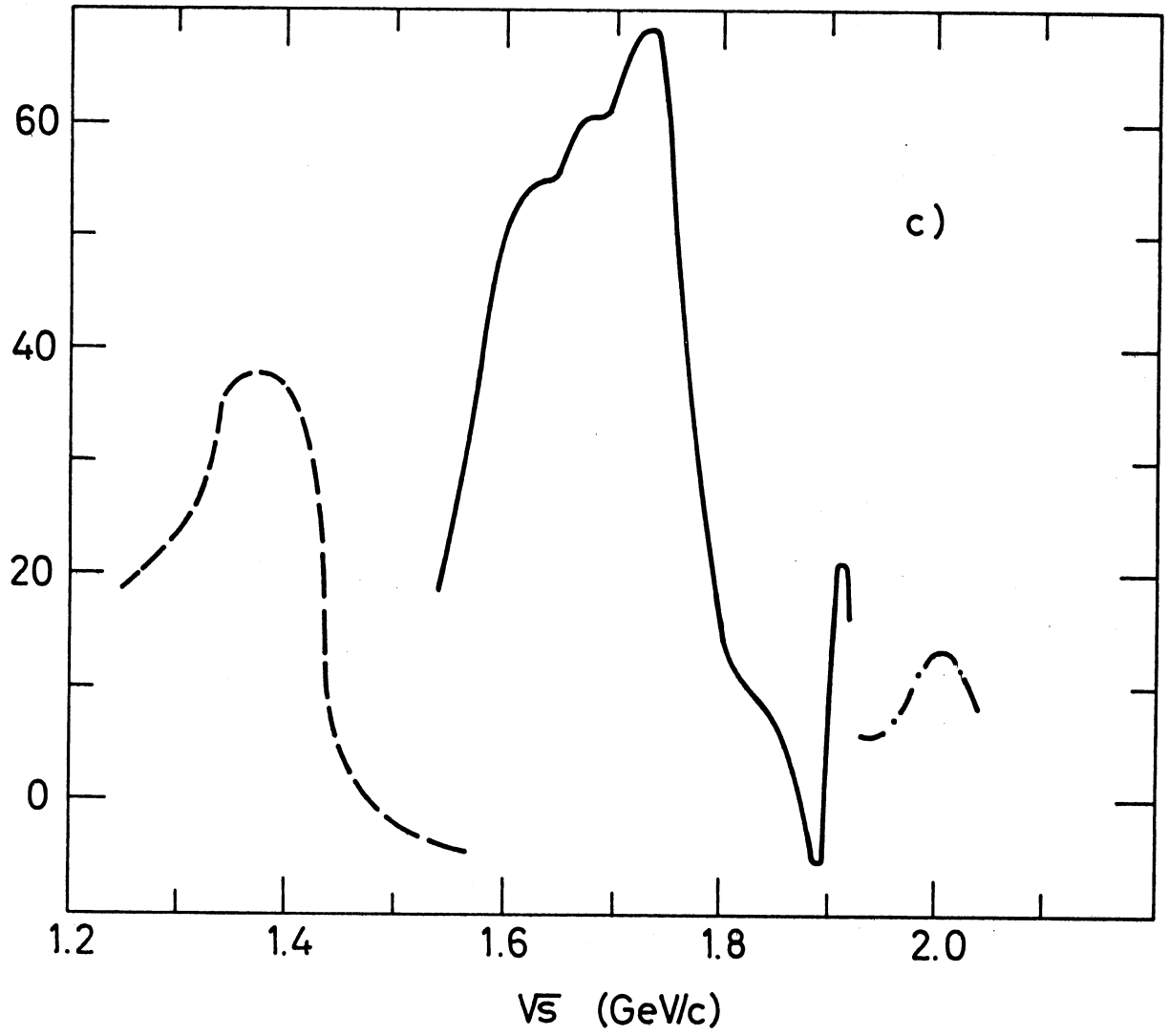

- Figure 2c -

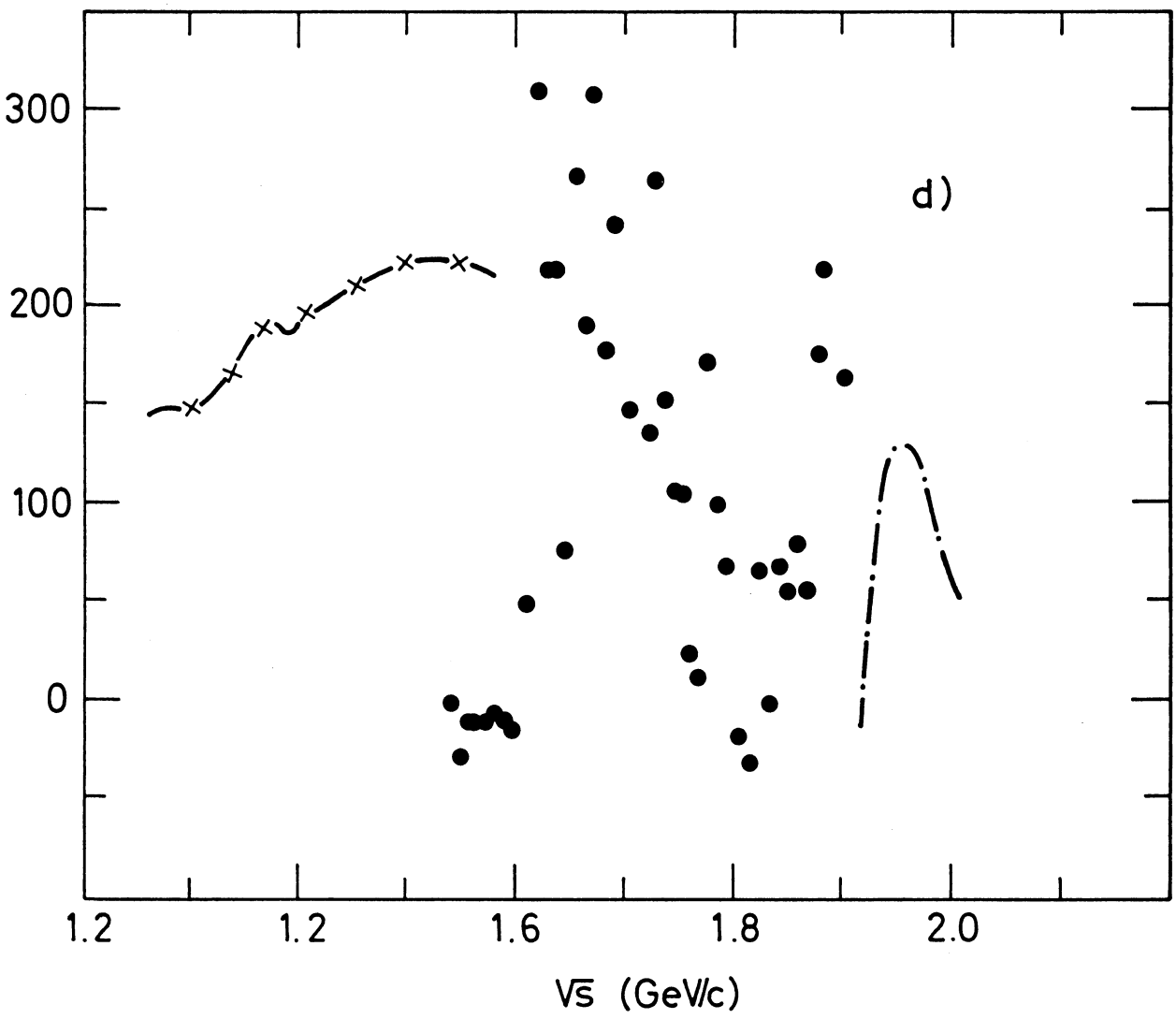

- Figure 2d -

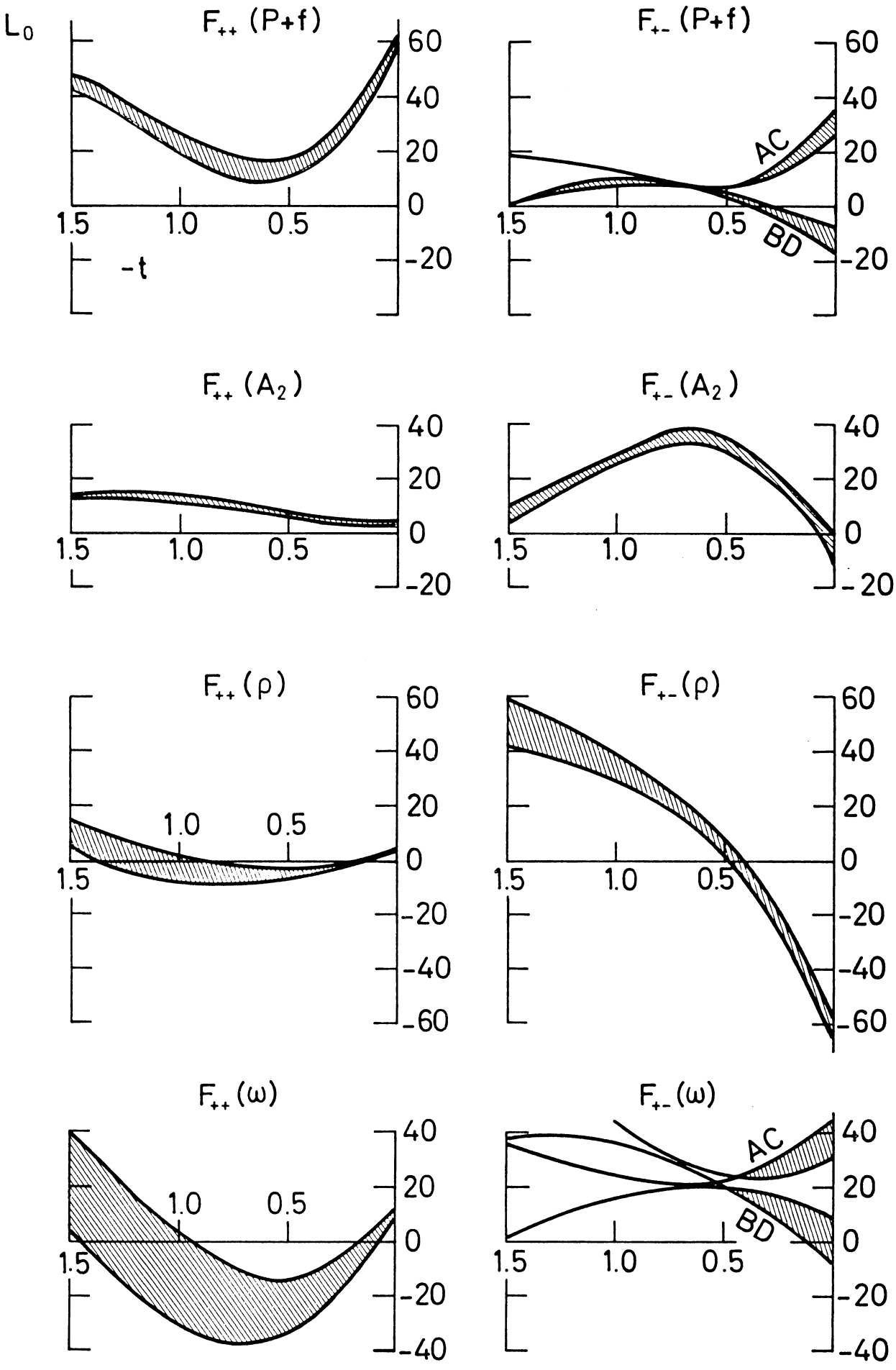

- Figure 3a -

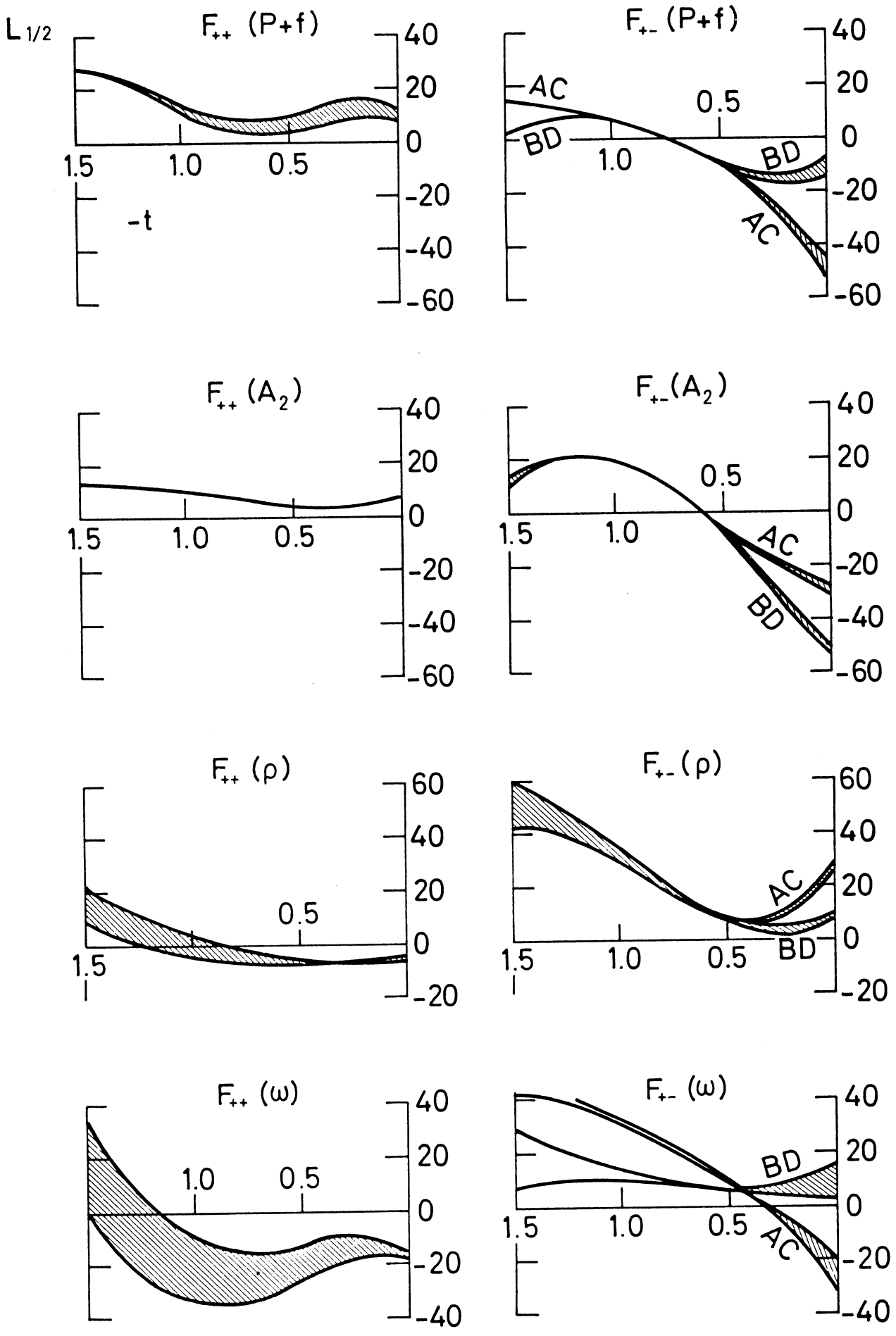

- Figure 3b -